

Article

Separation and Comprehensive Recovery of Cobalt, Nickel, and Lithium from Spent Power Lithium-Ion Batteries

Liwen Ma^{1,2}, Xiaoli Xi^{1,3,*}, Zhengzheng Zhang³ and Zhe Lyu⁴

¹ Key Laboratory of Advanced Functional Materials, Ministry of Education, Faculty of Materials and Manufacturing, Beijing University of Technology, Beijing 100124, China; maliwen@bjut.edu.cn

² National Engineering Laboratory for Industrial Big-Data Application Technology, Beijing University of Technology, Beijing 100124, China

³ Collaborative Innovation Center of Capital Resource-Recycling Material Technology, Beijing University of Technology, Beijing 100124, China; zhangzhengzheng@emails.bjut.edu.cn

⁴ Xiamen Tungsten Co., Ltd., Xiamen 361026, China; lv.zhe@cxtc.com

* Correspondence: xixiaoli@bjut.edu.cn

Abstract: The popularization of electric vehicles drives the extensive use of power lithium-ion batteries (LIBs) and their abandonment after retirement. Spent power LIBs have a high economic value because they contain valuable metals which need to be recovered. In this study, the separation and comprehensive recovery of valuable metallic elements, including Co, Ni, and Li, from spent power LIBs were realized by a hydrometallurgical process of “calcination–leaching–synergistic extraction–synthesis”. The results showed that, under the optimal conditions, the extraction efficiencies of impurities, such as Al and Cu, by P204 were 91% and 90%, respectively. A P507–N235 synergistic system was proposed to extract Co over Ni and Li with the maximum synergistic coefficient of 12.6. The extraction efficiency of Co, Ni, and Li was 99.5%, 3.9%, and 9.7%, respectively, and the separation coefficients of $\beta(\text{Co}/\text{Ni})$ and $\beta(\text{Co}/\text{Li})$ were 200.6 and 300.3, respectively. Cobalt oxalate, nickel oxalate, and lithium carbonate were finally obtained. Comprehensive recovery of valuable metals was realized, and the total recovery efficiency of Li, Ni, and Co was 84.1%, 93.1%, and 96.5%, respectively. This study provides positive significance for the improvement of cobalt extraction technology and comprehensive recycling efficiency of spent power LIBs.

Keywords: spent power lithium-ion batteries; cathode active materials; acid leaching; synergistic extraction; recovery



Citation: Ma, L.; Xi, X.; Zhang, Z.; Lyu, Z. Separation and Comprehensive Recovery of Cobalt, Nickel, and Lithium from Spent Power Lithium-Ion Batteries. *Minerals* **2022**, *12*, 425.

<https://doi.org/10.3390/min12040425>

Academic Editor: Eric D. van Hullebusch

Received: 15 February 2022

Accepted: 27 March 2022

Published: 30 March 2022

Publisher's Note: MDPI stays neutral with regard to jurisdictional claims in published maps and institutional affiliations.



Copyright: © 2022 by the authors. Licensee MDPI, Basel, Switzerland. This article is an open access article distributed under the terms and conditions of the Creative Commons Attribution (CC BY) license (<https://creativecommons.org/licenses/by/4.0/>).

1. Introduction

In recent years, electric vehicles (EVs) have been developed and popularized because of their potential to reduce green-house gases and decrease dependence on oil. According to the International Energy Agency, the production of EVs is predicted to reach 44 million vehicles per year by 2030, and the predicted demand for nickel (Ni) and cobalt (Co) for EVs in 2030 is expected to be 1.1 and 0.3 million tons, respectively, based on reports from the British Geological Survey [1]. The widespread use of lithium-ion batteries (LIBs) and their limited service time lead to the generation of a large number of spent LIBs. It is, thus, predicted that the output of spent power LIBs is expected to increase from 10,700 tons in 2012 to 464,000 tons in 2025, with a compound annual growth rate of 59% [2]. Thus, these batteries need to be well treated.

LIBs are mainly composed of the shell, electrolyte, cathode electrode, separator, and negative electrode. Unfortunately, spent LIBs have harmful effects on the environment. The reaction of cathode materials with organic solvents or reducing agents produces toxic gases and heavy metal pollution. If the spent LIBs are not effectively treated, a large amount of solid waste is produced [3]. Moreover, spent LIBs contain a large number of valuable metals, e.g., Ni: 5–10%, Co: 20%, and Li: 5–7%. China is short of Co and Ni. Spent LIBs have high

recovery value. The Co content in the most widely used LIBs is up to 20%, while natural Co ore has a low grade of 0.01–0.20%. The spent LIB is an important secondary resource [4].

The recycling of spent LIBs is mainly concentrated on the recovery of valuable metals, such as Co, Ni, and Li, because these metals are rare metals and have higher value than Fe, Al, and Cu. The most commonly used recovery methods include hydrometallurgy, pyrometallurgy, and biological metallurgy [5,6]. Compared with pyrometallurgical or biological processes, the hydrometallurgical process offers higher purity of the final product, easier control of the reaction process, and less environmental pollution, which makes it a more competitive recovery technology for spent LIBs. Hydrometallurgical processes include the following four stages: pre-treatment; leaching; separation; and synthesis. Many studies have been carried out on the leaching of spent cathode active materials. Common leaching agents include inorganic acids (hydrochloric, sulfuric, nitric acid) and various organic acids, such as ascorbic, citric, malic, aspartic, oxalic, DL-maleic, succinic, tartaric, iminodiacetic, maleic, amino acid, and so on. The leaching efficiency of Co and Ni was 95% in most studies, and some even achieved 100% [7–12].

Chemical precipitation, ion exchange, solvent extraction, and electrochemical methods can be used to separate metal ions present in the leaching solution [13]. According to the difference of solubility or distribution coefficients between two insoluble solvents, the solvent extraction method realizes the extraction and separation of solutes from solvents. This method has advantages such as high efficiency, energy savings, easy-to-realize continuous operation, reagent recyclability, cost effectiveness, and so on; therefore, solvent extraction is considered as one of the most commonly used hydrometallurgical methods for recycling spent LIBs. A number of solvent extraction systems, including P204 (di-2-ethylhexyl phosphoric acid), P507 (PC-88A, 2-ethylhexyl phosphonic acid mono-2-ethylhexyl ester), and Cyanex 272 (bis-2,4,4-trimethylpentyl phosphinic acid), proved to be effective for metal separation from spent LIBs. They were proven to have good separation performance for Co or other elements from the leaching solution of spent LIBs [14,15]. It is noteworthy that some extraction systems with synergistic effects have more positive significance for metal separation, such as P204/TPB (tributyl phosphate), Versatic 10 (neodecanoic acid)/LIX 84-I (2-hydroxy-5-nonylacetophenone oxime), Cyanex272/PC-88A, Mextral 84H (2-ethylhexyl phosphonic acid mono (2-ethylhexyl) ester)/Versatic 10, and their effects are listed in Table 1. Clearly, synergistic extraction system can enhance the metal separation efficiency, and this is a trend of extraction research.

Table 1. Orthogonal experimental system for P204 extraction.

Extraction System	Effect
P204/TPB [16]	Extracts Mn from Co and Ni, extraction efficiency 98.7%
Versatic 10/LIX 84-I [17]	Extracts Ni from Li, Mn, and Co, extraction efficiency 98.3%
Versatic 10 acid/extral 984H [18]	Extracts Cu, Ni, Co, and Zn from Ca and Mg, extraction efficiency >90%
Cyanex272/PC-88A [19]	Extraction order Mn > Co » Li, maximum synergistic coefficients Co ²⁺ 3.48 and Mn ²⁺ 4.12
Mextral 84H/Versatic 10	Extraction of Ni
Mextral 84H/P204 [20]	Mextral 84H/Versatic 10 has no significant synergistic effect; Mextral 84H/P204 system, synergistic coefficient 3.40
P507–N235 [21]	Extracts V and Mo from Al and Mg, extraction efficiency >99%
P507–N235 [22]	Extracts V, extraction efficiency >95%
P204–N235 [23]	Extracts Fe, extraction efficiency >97%

Moreover, a number of synergistic solvent extraction systems were developed to recover Ni, Co, Zn, and Cu from sulfuric acid and chloride leach solutions, which show great prospects for industrial application [24]. Compared with other metals, due to the similar properties of Co and Ni, there is a greater need to improve Co extraction through the improvement of the synergistic extraction system. The extraction mechanism of Co for traditional acidic extractants, such as P507, is the ion-exchange mechanism. Hydrogen ions on P507 are exchanged with Co ions in the solution. It becomes necessary to perform saponification to stabilize the pH of the system. Notably, the nitrogen donor group can extract acid; therefore, the acidic systems mixed with the nitrogen donor group can form a saponification-free extraction system. Moreover, this type of system was found to produce strong, synergistic effects on the extraction of certain metal ions. For example, the P507–N235 (trioctyl tertiary amine) system was used to separate rare earth elements or vanadium [21,22,25,26]. However, this system has rarely been used for Co extraction.

Compared with other spent LIBs for electronic devices, there is no essential difference for spent power LIBs in the composition and recovery process, but they have the advantage of large-scale recycling due to the popularity of EVs. As spent power LIBs are larger in number and more stable in composition, they can be recycled more conveniently. There are two recycling strategies: to prepare high-value-added materials, such as $\text{LiNi}_{0.8}\text{Co}_{0.15}\text{Al}_{0.05}\text{O}_2$, as in our previous work [27] or to realize efficient and comprehensive recycling through a more effective extraction system and optimized process route, as in this study. In this study, the hydrometallurgical process of recovering valuable metal elements, such as Co, Ni, and Li, from spent power LIBs was proposed. The process includes calcination, leaching, extraction separation, and synthesis of the final products. The non-saponification P507–N235 system was proposed for the separation of Co and Ni, and its synergistic effects were evaluated. This study provides a reference for optimizing the comprehensive recycling process of spent power LIBs.

2. Materials and Methods

2.1. Experimental Materials and Reagents

The spent power LIB studied herein was the retired battery of a Mercedes-Benz S400 Hybrid obtained from Beijing Jinyu Mangrove Environmental Protection Technology Co., Ltd., Beijing, China. The disassembly process of its internal battery unit is shown in Figure 1a–c, and the obtained cathode plate is shown in Figure 1d. The separation of cathode active materials was achieved by partially dissolving the aluminum (Al) foil carrier. The cathode plates were cut into small pieces of 10 cm × 10 cm size and were soaked in NaOH solution (100 mL, 2 mol L^{−1}) at room temperature for 1 min, and the Al foil carrier (Figure 1e) and black spent cathode active material (Figure 1f) were obtained. The black spent cathode active material (0.20 g, accurate to 0.0001 g) was put in a 100 mL small beaker and then freshly prepared aqua regia (20 mL) was added. The beaker was then covered with a surface dish, and the sample was boiled and steamed to wet salt. After cooling to room temperature, aqua regia (3 mL) was added and boiled until all the samples were digested. After cooling, the sample was transferred into a 100 mL volumetric flask for inductively coupled plasma optical emission spectroscopy (ICP-OES) measurement (PerkinElmer, Waltham, MA, USA).

P507, N235, P204, and kerosene of industrial premium grade were purchased from Luoyang Aoda Chemical Co., Ltd. (Luoyang, China). All inorganic chemicals used, such as HCl, H₂SO₄, NaOH, Na₂CO₃, H₂O₂, and oxalic acid, were analytical grade and purchased from Tianjin Fuchen Chemical Reagent Co., Ltd. (Tianjin, China).

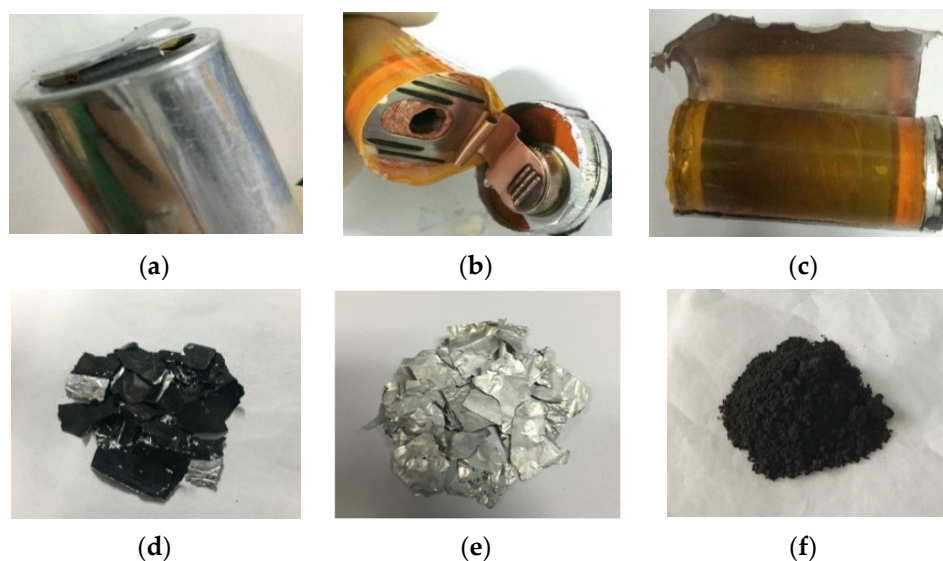


Figure 1. Spent power LIB: (a) battery unit, (b) battery cover opened, (c) shell pull out, (d) cathode plate, (e) aluminum foil, and (f) cathode active material.

2.2. Leaching Procedure

The cathode active material was leached by sulfuric acid with hydrogen peroxide as reducing agent. Hydrogen peroxide reduced Co^{3+} in the solution to Co^{2+} . The leaching conditions were as follows: $2 \text{ mol L}^{-1} \text{ H}_2\text{SO}_4$, solid–liquid ratio of $7.5 \text{ g} \cdot 100 \text{ mL}^{-1}$, $85 \text{ }^\circ\text{C}$, 50 min, and $V_{(\text{H}_2\text{O}_2)} = 5\%$. The leaching efficiencies of Co, Ni, and Li are 100% according to the previous study [12]. The leaching solution contained about $8.8 \text{ g L}^{-1} \text{ Co}$, $44.7 \text{ g L}^{-1} \text{ Ni}$, $4.7 \text{ g L}^{-1} \text{ Li}$, $1.3 \text{ g L}^{-1} \text{ Al}$, and $2.1 \text{ g L}^{-1} \text{ Cu}$.

2.3. Solvent Extraction by P204

P204 was employed to extract Al and Cu during the first stage. Orthogonal experiment was conducted for P204 extraction [28,29]. Four factors were selected: pH, saponification rate, volume ratio of organic phase to aqueous phase ($V_o:V_a$), and volume ratio of P204 to kerosene ($V_{\text{P204}}:V_{\text{kerosene}}$), which were represented by the notations A, B, C, and D, respectively. Three levels were selected for each factor, and the orthogonal experiment was designed according to Table 2. The leaching solution was modified to the desired pH by adding either H_2SO_4 (1.5 mol L^{-1}) or NaOH (1.0 mol L^{-1}) before P204 solvent extraction. The extractants were saponified by adding a sufficient quantity of a solution of NaOH to neutralize the desired quantity of the extractant. Saponification stabilized the acidity of the raffinate which promoted the extraction. For experiment No. 1, the initial pH was adjusted to 3, and the organic phase was composed of 14.3 vol% P204 and kerosene ($V_{\text{P204}}:V_{\text{kerosene}} = 1:6$). NaOH solution (6.5 mL , 1 mol L^{-1}) and P204 (50 mL , 14.3 vol%) were mixed in a separating funnel and then mechanically shaken for 1 min. The upper organic solution was the saponified P204 organic phase. The saponification rate was calculated as 30% according to Equation (1), as follows:

$$R_s = (n_{\text{NaOH}} \cdot V_{\text{NaOH}}) / (V_{\text{P204}} \cdot V_{\text{P204}}\% \cdot \rho_{\text{P204}} / M_{\text{P204}}) \times 100\% \quad (1)$$

where R_s is saponification rate (%), which represents the percentage of the mole amount of hydrogen available for ion exchange in P204 replaced with Na; n_{NaOH} is the moles concentration of NaOH (mol L^{-1}); V_{NaOH} is the volume of NaOH (mL); V_{P204} is the volume of P204 system (mL); ρ_{P204} is the density of P204, 0.973 g cm^{-3} ; $V_{\text{P204}}\%$ is the volume ratio of P204 system; and M_{P204} is molecular mass of P204, $322.48 \text{ g mol}^{-1}$.

Table 2. Orthogonal experimental conditions for P204 extraction.

Level	A Saponification Rate/%	B pH	C $V_o:V_a$	D $V_{P204}:V_{kerosene}$
1	30	3	1:6	1:6
2	50	4	1:4	1:4
3	70	4.5	1:2	1:2

Solvent extraction experiments were carried out in separating funnels (250 mL) with organic phase (20 mL) and aqueous phase (120 mL) ($V_o:V_a = 1:6$) by mechanically shaking for 10 min and then the two phases were separated after phase disengagement within 5 min. The concentration of Co, Ni, and Li in the aqueous phase was analyzed by ICP-OES, and the concentration of metals in the loaded organic phase was calculated by mass balance. In the stripping process, the loaded organic phase and strippant (2 mol L^{-1} HCl, $V_o:V_a = 1:2$) were mixed in separating funnels (250 mL) with mechanical shaking at room temperature for 5 min and separated after phase disengagement within 5 min. The computation method of metal concentration in the aqueous phase and the organic phase was described previously. The operation of experiment No. 2 and experiment No. 3 was similar to that of experiment No. 1, and their extraction conditions are listed in Table 2.

2.4. Solvent Extraction by P507–N235

N235 was added into P507 to obtain a P507–N235 system for Co extraction. It is noteworthy that this system does not need saponification and can shorten the process. Under the conditions, including pH 4, saponification rate 70%, $V_{P204}:V_{kerosene} = 1:2$, and $V_o:V_a = 1:2$, the leaching solution, after the removal of Al and Cu impurities, was treated with P507–N235 system to extract Co. Single-factor experiments were employed in this stage. The effect of different ratios of $V_{P507-N235}:V_{kerosene}$ was investigated. The initial pH was adjusted to 2.5, the organic phase was composed of different volume ratios of P507–N235 to kerosene ($V_{P507-N235}:V_{kerosene}$ varied from 1:1–1:5), and the volume ratio of P507 to N235 ($V_{P507}:V_{N235}$) was 3:7. Solvent extraction experiments were carried out in separating funnels (250 mL) with the 80 mL organic and 20 mL aqueous phases ($V_o:V_a = 4:1$) by mechanically shaking for 20 min and then the two phases were separated after phase disengagement within 5 min. The concentration of Co, Ni, and Li in the aqueous phase was analyzed by ICP-OES, and the concentration of metals in the loaded organic phase was calculated by mass balance. The effect of different, initial pHs (2–5) of aqueous phase and $V_o:V_a$ ratios (1:1–5:1) on Co, Ni, and Li extraction by P507–N235 system was studied by employing similar experimental operations to obtain the optimal conditions. In the single-factor experiment, the fixed experimental conditions were as follows: $V_{P507}:V_{N235} = 3:7$, $V_{P507-N235}:V_{kerosene} = 1:3$, $V_o:V_a = 4:1$, pH = 2.5, and $t = 20$ min.

The synergistic effect of P507–N235 system was also studied. Under the conditions of $V_{P507-N235}:V_{kerosene} = 1:3$, $V_o:V_a = 4:1$, pH = 2.5, and $t = 20$ min, the Co extraction ability at different $V_{P507}:V_{N235}$ ratios ($V_{P507}:V_{N235}$ varied from 1:9 to 9:1) was investigated. For comparative analysis, the non-saponified, single P507 system (P507 vol% in kerosene varied from 10–90%) and single N235 system (N235 vol% in kerosene varied from 10–90%) were subjected to the same experimental procedure, respectively. The distribution ratio, extraction efficiency, and separation coefficient of metal ions were calculated according to Equations (2)–(6):

$$D = C_o/C_a \quad (2)$$

where D is distribution ratio; C_o is the total concentration of metallic element in organic phase (g L^{-1}); and C_a is the total concentration of metallic element in aqueous phase (g L^{-1}).

$$E = M_o/(M_a + M_o) \times 100\% \quad (3)$$

$$= D/(D + V_a/V_o) \times 100\% \quad (4)$$

$$= D/(D + 1/R) \times 100\% \quad (5)$$

where E is extraction efficiency (%); M_o is the total mass of metallic element in organic phase (g); M_a is the total mass of metallic element in aqueous phase (g); and R is the volume ratio of the organic phase to aqueous phase.

$$\beta = D_M/D_N \quad (6)$$

where β is separation coefficient for element M to element N ; D_M and D_N are the distribution ratios of element M and element N under the same extraction conditions, respectively. For the extraction system of components A and B , the synergistic coefficient can be calculated by using Equation (7), as follows:

$$S = D_{A+B}/(D_A+D_B) \quad (7)$$

where S is synergistic coefficient, D_{A+B} is the distribution ratio in $A+B$ system, and D_A or D_B is the distribution ratio in A system or B system under the same conditions.

2.5. Synthesis of Products

After extraction under the optimal conditions, the P507–N235 organic phase was stripped by 1 mol L^{-1} HCl and 1 mg L^{-1} oxalic acid ($V_{\text{organic phase}}:V_{\text{oxalic acid}}:V_{\text{HCl}} = 2:4:3$) at $30 \text{ }^\circ\text{C}$, and cobalt oxalate precipitated in the stripping solution. The raffinate after P507–N235 extraction contained Ni and Li. Addition of the optimal dosage of oxalic acid (150 mg) to raffinate (1 mL) at $25 \text{ }^\circ\text{C}$ led to the precipitation of nickel oxalate; however, Li remained in the raffinate. Lithium carbonate was precipitated by sodium carbonate after Ni precipitation at $95 \text{ }^\circ\text{C}$. The dosage ratio was 50 mg of sodium carbonate to 1 mL of raffinate. All precipitates were dried at $60 \text{ }^\circ\text{C}$.

2.6. Analysis and Characterization

The concentrations of various metal ions in the solutions were determined by ICP-OES (Optima 7000DV, PerkinElmer, Waltham, MA, USA). The pH of the aqueous solutions was measured using a pH meter (S220-Bio, Mettler Toledo, Zurich, Switzerland). The structures, morphology, and composition of the spent active material or recovered products were identified by X-ray diffraction (XRD, 7000, Shimadzu, Japan), scanning electron microscopy (SEM, Quanta FFG650, FEI Company, Hillsborough, Oregon, USA), and energy-dispersive spectrometry (EDS, Quanta FFG650 system, FEI Company, Hillsborough, OR, USA). The functional groups in extracts were determined by infrared (IR) spectroscopy (Nicolet-6700, Thermo Nicolet Corporation, Madison, WI, USA). The spent cathode active materials for calcination were analyzed by thermogravimetry (TG, Labsys Evo, Setaram, Lyon, France).

3. Results and Discussion

3.1. Flow Chart of the Process

Figure 2 shows the flow chart of the recovery process for the cathode plates of spent power LIBs, presenting the main process parameters and the recovery efficiency of the main elements for each step. This process of “calcination–leaching–synergistic extraction–synthesis” was aimed to dissolve the carrier and destroy the structure of spent cathode material by calcination and then to leach Co, Ni, Li, Cu, and Al by H_2SO_4 . Further, the process removes Cu and Al by P204 extraction and aids in extraction of Co with the synergistic extraction system P507–N235. Next, the organic phase is stripped off to obtain cobalt oxalate, and the raffinate is precipitated twice to obtain nickel oxalate and lithium carbonate. The total recovery efficiency of each metallic element can be calculated by multiplying the recovery efficiency at each step. The total recovery efficiency of Li, Ni, and Co was 84.1%, 93.1%, and 96.5%, respectively. For each step, the specific research process is presented in the following sections.

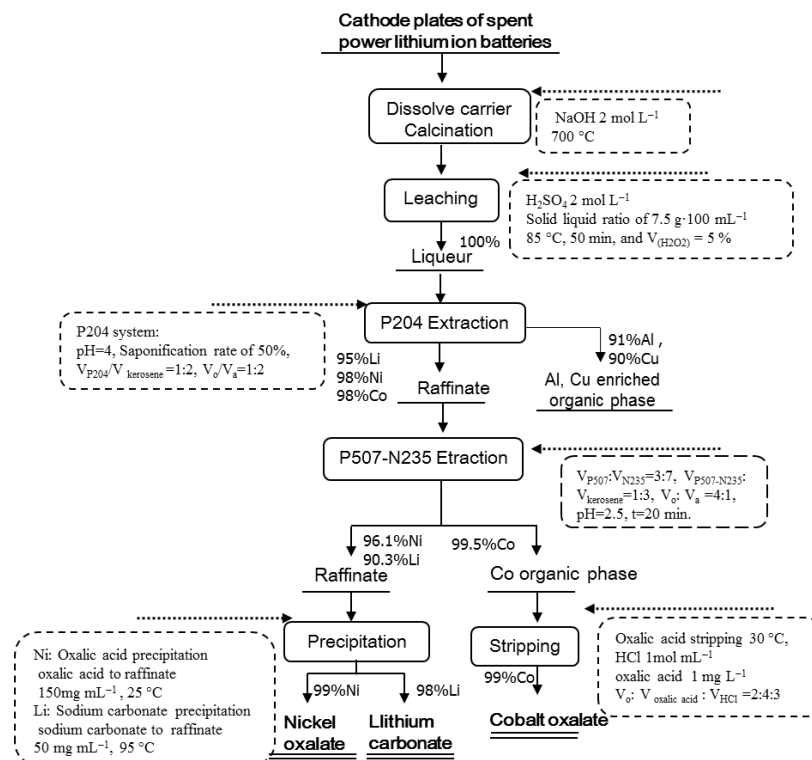


Figure 2. Flow chart of the recovery process route.

3.2. Composition and Structure of Spent Cathode Active Materials

The XRD pattern of the cathode active material of spent power LIB shows that the active material was black, layered lithium nickel cobalt oxide $\text{Li}(\text{Ni}_x\text{Co}_{1-x})\text{O}_2$, as shown in Figure 3. The contents of Li, Ni, and Co in the spent cathode active materials were found to be 6.26%, 59.65%, and 11.67%, as detected by ICP-OES.

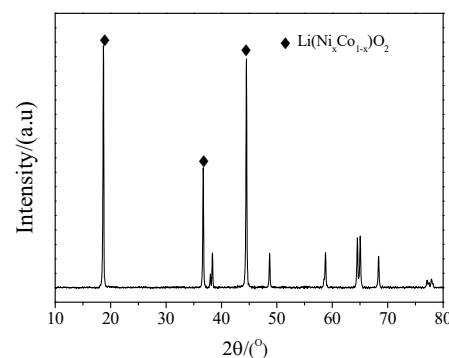


Figure 3. XRD patterns of the spent cathode active materials.

3.3. Calcination of Spent Cathode Active Materials

Calcination was used to destroy the layered structure and decompose the active material. The changes during the calcination are shown in Figure 4. Figure 4a shows the TG differential scanning calorimetry (DSC) curves of the cathode active material calcined at 25–500 °C. The TG curve shows that the mass of the cathode active material was decreasing. The DSC curve shows the presence of two endothermic peaks at about 60.6 °C and 133.1 °C, respectively, which were mainly attributed to the removal of the gas that was formed by the heat absorption of free water on the surface and combined water of the sample. An exothermic peak was observed at 210.4 °C, which was attributed to the decomposition of the residual electrolyte. There was an exothermic peak at 365.5 °C, which corresponded to the decomposition of the binder. When the temperature increased,

the decomposition rate accelerated. Further, an exothermic peak was also observed at 438.1 °C, which was attributed to the primary decomposition of the cathode active material. Figure 4b shows the TG DSC curves of the cathode active material calcined at 25–750 °C. There was a maximum exothermic peak at 593 °C, and a weight loss occurred between 593 and 700 °C. It corresponded to the complete decomposition of the cathode active material, and the layered structure was destroyed.

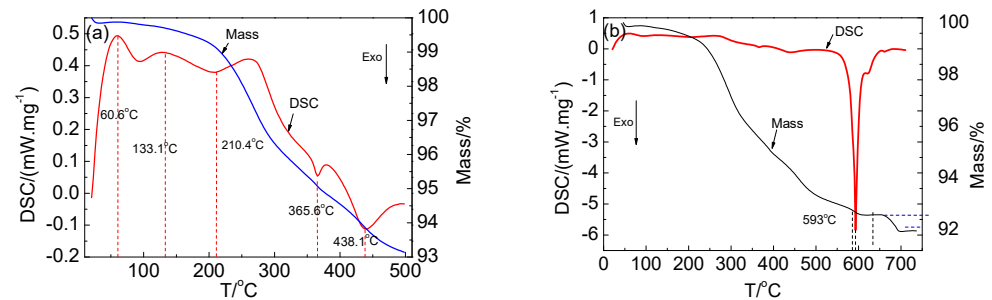


Figure 4. TG and DSC curves of the cathode active material: (a) 25–500 °C and (b) 25–750 °C.

The XRD patterns of the spent cathode active materials calcined at different temperatures for 2 h are shown in Figure 5. The cathode active material did not decompose, and it remained as lithium nickel cobalt oxide $\text{Li}(\text{Ni}_x\text{Co}_{1-x})\text{O}_2$ at a temperature below 400 °C. However, it began to decompose and form $\text{Li}_{0.4}\text{Ni}_{1.6}\text{O}_2$ at $400\text{ °C} < T \leq 500\text{ °C}$. Furthermore, the cathode active material decomposed into NiO, CoO, and other substances at above 500 °C. It indicates that the high temperature destroyed the layered structure of the active material. There was no layered $\text{Li}(\text{Ni}_x\text{Co}_{1-x})\text{O}_2$ phase in the spent cathode active material at above 600 °C.

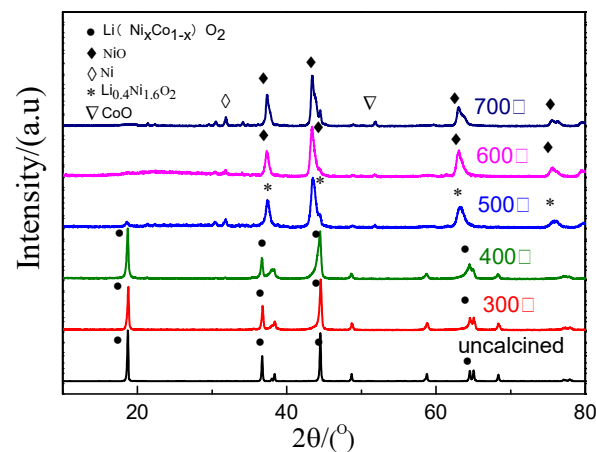


Figure 5. XRD patterns of cathode active material before and after calcination.

The uncalcined spent cathode active material and the sample calcined at 700 °C were analyzed by SEM and EDS, and the corresponding results are shown in Figure 6. After calcination, the particle size of the material became smaller; however, the composition remained unchanged. Small particle size was conducive to the subsequent acid leaching.

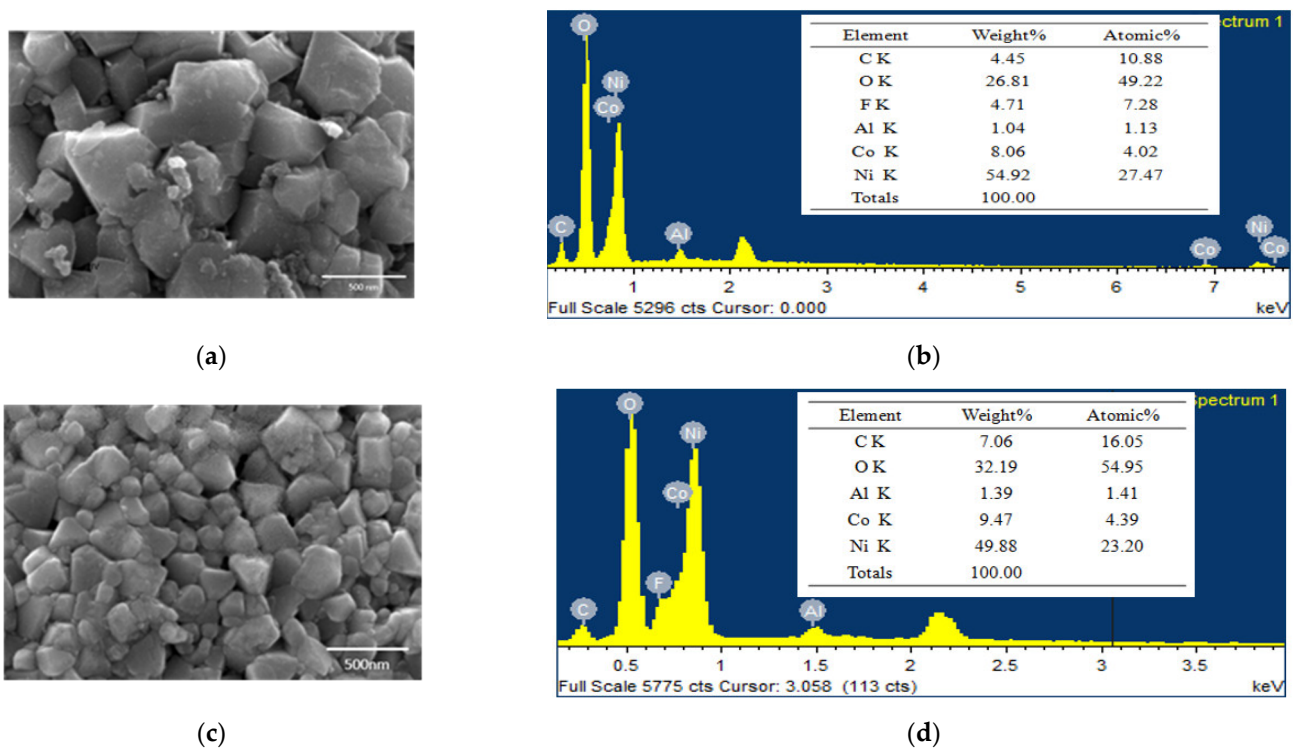


Figure 6. SEM images and EDS pattern of cathode active material: (a,b) uncalcined and (c,d) calcined at 700 °C.

3.4. Extraction of Al and Cu by P204

The cathode active material was leached using sulfuric acid with hydrogen peroxide. The leaching solution consisted of Co, Ni, Li, Al, and Cu. The extraction of Al and Cu by P204 was studied by orthogonal experiments to find out the optimal condition combination, and the results are presented in Table 3. In order to facilitate the analysis, the involved symbols and expressions were first defined. Then, k_{1FAI} was taken as the average value of test indexes (Al extraction efficiency) at level 1 for the different factors; F is referred to A, B, C, and D. Accordingly, k_{1FCu} was taken as the average value of test indexes (Cu extraction efficiency) at level 1 for different factors. The range R was calculated as $R_{Al} = \max(k_{1AAI}, k_{1BAI}, k_{1CAI}, k_{1DAI}) - \min(k_{1AAI}, k_{1BAI}, k_{1CAI}, k_{1DAI})$. According to the value range of R, the order of influencing factors could be inferred. Table 3 illustrates that, according to the order of R_{Al} and R_{Cu} from large to small, the influencing order of different factors was $D > C > B > A$ for extraction of both Al and Cu. Therefore, the order of influencing factors was $V_{P204}:V_{kerosene}, V_o:V_a$, saponification rate, and pH. Figure 7 shows the relationship between the factor levels and the average value of extraction efficiency of Al or Cu, i.e., the indexes k (k represents $k_{1FAI}, k_{2FAI}, k_{3FAI}$ or $k_{1FCu}, k_{2FCu}, k_{3FCu}$). According to the maximum value of k , the optimal condition of P204 extraction for Al was $A_2B_3C_3D_3$; that is, pH = 4, a saponification rate of 70%, $V_{P204}:V_{kerosene} = 1:2$, and $V_o:V_a = 1:2$. Similarly, the optimal condition of P204 extraction for Cu was $A_1B_2C_3D_3$; that is, pH = 3, a saponification rate of 50%, $V_{P204}:V_{kerosene} = 1:2$, and $V_o:V_a = 1:2$. Under the conditions of $A_1B_2C_3D_3$, the extraction efficiency of Al, Cu, Co, Ni, and Li was 91%, 90%, 2%, 2%, and 5%, respectively.

Table 3. Orthogonal experiment and experimental results of P204 extraction $L_9(3^4)$.

No.	A pH	B Saponification Rate	C $V_o:V_a$	D $V_{P204}:V_{kerosene}$	$E_{(Al)}/\%$	$E_{(Cu)}/\%$
1	3	30	1:6	1:6	14.05	16.83
2	3	50	1:4	1:4	18.04	23.55
3	3	70	1:2	1:2	84.46	59.17
4	4	30	1:4	1:2	63.12	76.96
5	4	50	1:2	1:6	39.90	34.87
6	4	70	1:6	1:4	58.97	30.06
7	4.5	30	1:2	1:4	34.09	59.14
8	4.5	50	1:6	1:2	66.06	49.35
9	4.5	70	1:4	1:6	20.85	34.60
k_{1FAI}	0.387	0.370	0.463	0.250		
k_{2FAI}	0.540	0.413	0.340	0.370		
k_{3FAI}	0.403	0.547	0.527	0.710		
R_{Al}	0.153	0.177	0.187	0.460		
k_{1FCu}	0.333	0.513	0.320	0.290		
k_{2FCu}	0.477	0.360	0.457	0.377		
k_{3FCu}	0.477	0.413	0.510	0.620		
R_{Cu}	0.144	0.153	0.190	0.330		

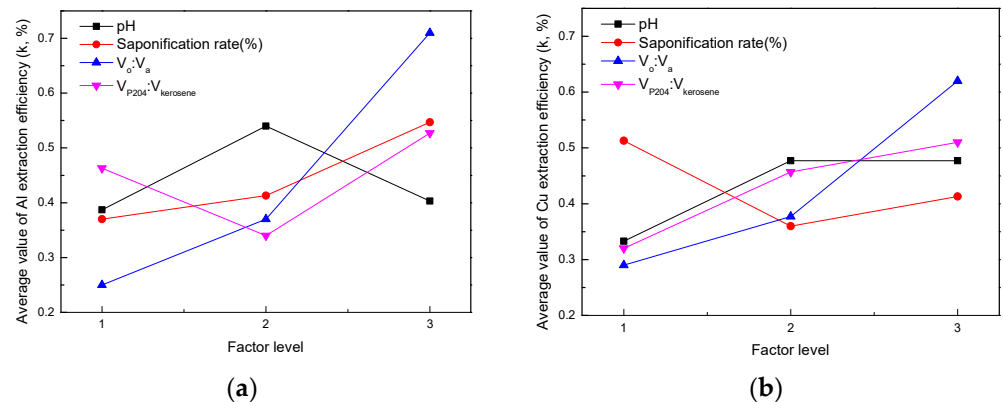


Figure 7. Relationship between factor level and the (a) Al extraction efficiency and (b) Cu extraction efficiency.

3.5. Extraction of Co by P507–N235 System

Conventionally, a P507 system is used for Co extraction. A P507 system also needs to be saponified before extraction. However, saponification adds waste water to the environment. Therefore, N235 was introduced to prepare a P507–N235 system for extraction without saponification, which simplifies the process flow. The P507–N235 system is a relatively novel extraction system. The single-factor condition experiments were adopted to determine the effect of different factors.

3.5.1. Effect of $V_{P507-N235}:V_{kerosene}$

The effect of different $V_{P507-N235}:V_{kerosene}$ ratios on the extraction of Co, Ni, and Li by P507–N235 was studied, as shown in Figure 8. Figure 8a shows that, when the $V_{P507-N235}:V_{kerosene}$ ratio was 1:3, the extraction efficiency of Co reached the maximum of 98%. Figure 8b shows that the largest separation coefficients of $\beta_{(Co/Ni)}$ and $\beta_{(Co/Li)}$ were also obtained at $V_{P507-N235}:V_{kerosene} = 1:3$.

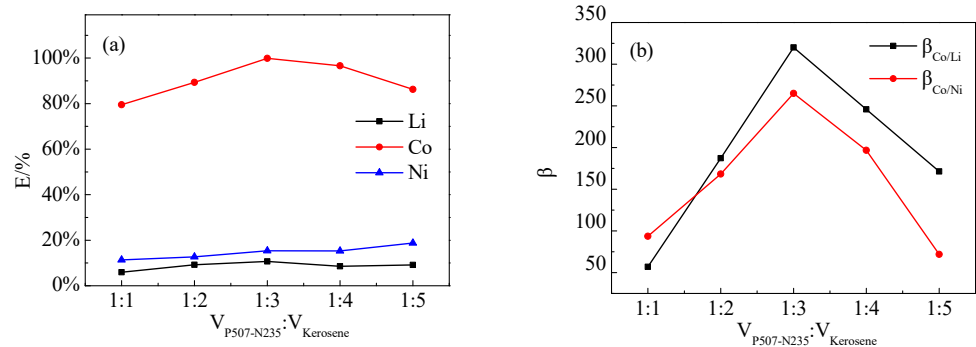


Figure 8. Effect of $V_{P507-N235}:V_{kerosene}$ ratio on: (a) extraction efficiency and (b) separation coefficient ($V_{P507}:V_{N235} = 3:7$, $V_o:V_a = 3:1$, $pH = 4.0$).

3.5.2. Effect of pH

The effect of a different, initial pH of the aqueous phase on the extraction of Co, Ni, and Li by P507–N235 was studied (Figure 9). When pH was 2.5, the Co extraction efficiencies, i.e., $\beta_{(Co/Ni)}$ and $\beta_{(Co/Li)}$, reached the maximum. Notably, H^+ on P507 was ion-exchanged with Co^{2+} in the extraction process; therefore, the pH of the aqueous phase was continuously reduced, and the extraction efficiency of Co was also reduced. The extraction efficiency was stable under the condition of low pH, which indicates that N235 has the ability to extract acid and can stabilize the pH of the solution, as shown in Equation (8).

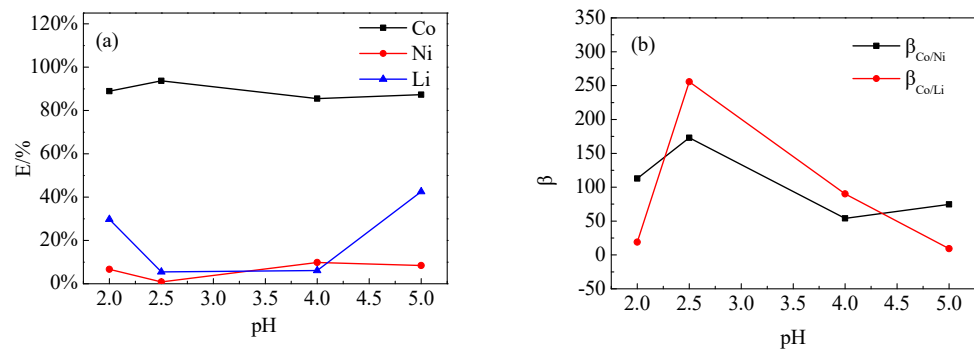


Figure 9. Effect of pH on (a) extraction efficiency and (b) separation coefficient ($V_{P507-N235}:V_{kerosene} = 1:3$, $V_{P507}:V_{N235} = 3:7$, $V_o:V_a = 3:1$).

3.5.3. Effect of $V_o:V_a$

The effect of different $V_o:V_a$ ratios on the extraction of Co, Ni, and Li by P507–N235 was studied, as shown in Figure 10. The Co extraction efficiencies, $\beta_{(Co/Ni)}$ and $\beta_{(Co/Li)}$, reached the maximum when the ratio was 4:1.

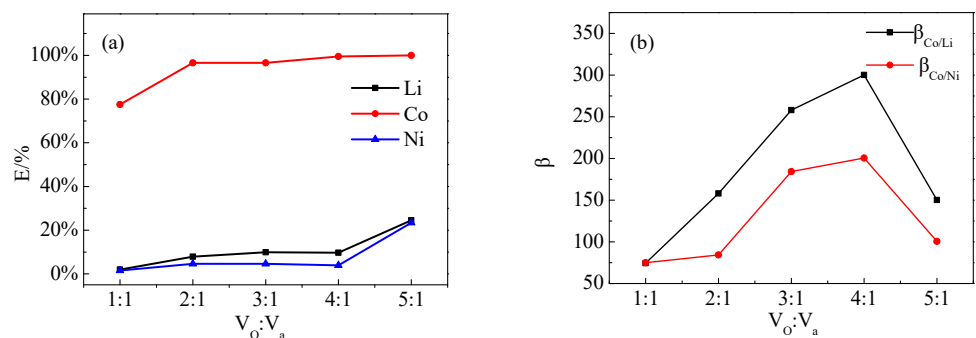


Figure 10. Effect of $V_o:V_a$ on (a) extraction efficiency and (b) separation coefficient ($V_{P507-N235}:V_{kerosene} = 1:3$, $V_{P507}:V_{N235} = 3:7$, $pH = 2.5$).

3.5.4. Synergistic Effect of P507–N235 System

Under the above-mentioned optimal conditions, the effect of different $V_{P507}:V_{N235}$ ratios on the distribution ratio of Co (D_{Co}) and the synergistic effect of the P507–N235 system were studied, and the corresponding results are shown in Figure 11. The results indicate that D_{Co} was very low for the single N235 system and non-saponified single P507 system. However, D_{Co} first increased and then decreased in the P507–N235 system with the increase of N235 volume ratio. When volume proportion $X(P507) = 0.3$, the D_{Co} reached the maximum of 13.7. According to Equation (6), the maximum synergistic coefficient in the P507–N235 system was 12.6, which indicates that the extraction system showed significant synergistic effect.

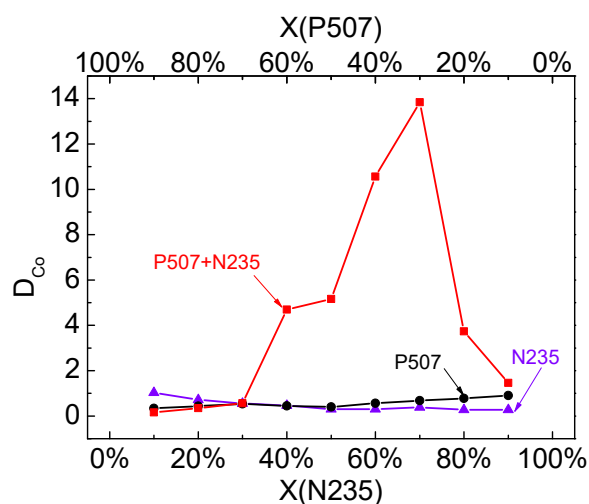


Figure 11. D_{Co} in P507 system, N235 system, and P507–N235 system ($V_{P507-N235}:V_{kerosene} = 1:3$, $V_o:V_a = 4:1$, $pH = 2.5$).

In summary, the optimal conditions for a P507–N235 system are $V_{P507}:V_{N235} = 3:7$, $V_{P507-N235}:V_{kerosene} = 1:3$, $V_o:V_a = 4:1$, $pH = 2.5$, and $t = 20$ min. Under these conditions, the maximum synergistic coefficient is 12.6, the extraction efficiency of Co is 99.5%, that of Ni and Li is 3.9% and 9.7%, respectively, and the separation coefficients of $\beta_{(Co/Ni)}$ and $\beta_{(Co/Li)}$ are 200.6 and 300.3, respectively.

3.5.5. Extraction Mechanism of P507–N235 System

The IR spectra of P507, N235, and the P507–N235 system are shown in Figure 12. N235 is a tertiary amine extractant, and the active group is tertiary amine group. Figure 12A shows the peak at 1097 cm^{-1} , which is the characteristic peak of basic group of N235. The peak at 1197 cm^{-1} shown in Figure 12B is the characteristic peak of the P=O bond in P507. When P507 and N235 were mixed according to the optimal volume ratio of 3:7, as shown in Figure 12C, the characteristic peak of the P=O bond in P507 shifted to around 1161 cm^{-1} , and the characteristic peak of N235 shifted to around 969 cm^{-1} , indicating that the two extractants exhibited a strong acid–base coupling effect in the mixing process. Owing to the influence of the extractant N235, the intensity of the characteristic peak of P507 also decreased, and a peak appeared near 1041 cm^{-1} , which may be due to the formation of associated molecules during the dissolution of the two extractants in kerosene. P507 and N235 contain N and O, which may provide lone pair electrons and form chemical bonds with H atoms [25]. P507 and N235 may undergo Reaction (8). P507: abbreviated as HA N235: abbreviated as R_3N .



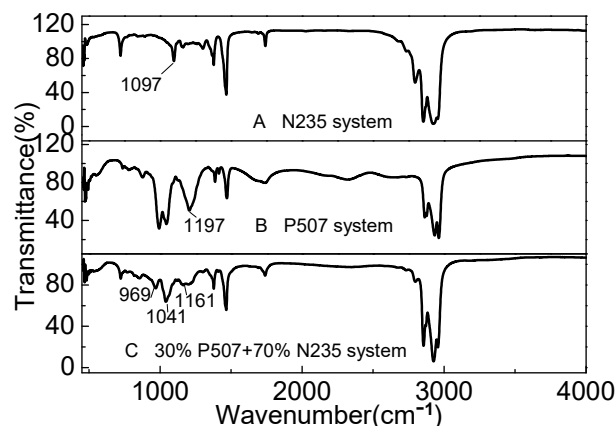


Figure 12. IR spectra of (A) N235, (B) P507, and (C) P507–N235 system ($V_{\text{extractant}}: V_{\text{kerosene}} = 1:3$).

The IR spectra before and after Co extraction by the P507–N235 system are shown in Figure 13. The peaks fluctuated between 3250 and 3750 cm^{-1} , which indicates the presence of an aqueous phase. After extraction, the P=O bond moved to low frequency, the peak increased slightly, and the peak became sharp. It is possible that the coordination between Co and extractants altered the symmetry and led to the change in the dipole moment of the P=O bond. The characteristic peak of the tertiary amine group of N235 was weakened after extraction, indicating that the tertiary amine group participated in the reaction.

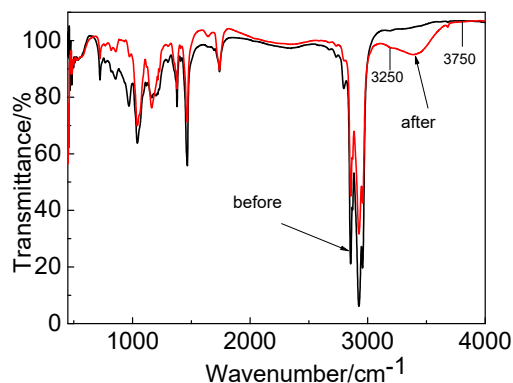


Figure 13. IR spectrogram before and after extraction by P507–N235 system.

In a chlorine-containing system, the chloride ion can form the complex CoCl_4^{2-} with Co^{2+} , as Co^{2+} has empty orbitals and Cl^- has high charge density. N235 can react with HCl and CoCl_4^{2-} in the acidic system. The reaction is represented as Equations (9) and (10).



Analysis of Figures 12 and 13 indicates that the main reaction during the extraction process in this P507–N235 system was Reaction (11). P507 and N235 aid in synergistic extraction of Co, which improves the separation between Co and Ni.

However, in sulfate media, Co cannot form coordination anion, because sulfate SO_4^{2-} is already a coordination polyhedron with low charge density and stable structure; thus, it is difficult to coordinate with other metallic ions, such as Co^{2+} . Therefore, a P507–N235 system in sulfate media extracts Co in a similar way to the single P507 and has no synergistic effect [30].



3.6. Synthesis of Co, Ni, and Li Products

After extraction by a P507–N235 system under the optimal conditions, the Co-loaded organic phase was stripped by oxalic acid mixed with HCl to obtain precipitate with the precipitation efficiency of 99%. The precipitate was analyzed by XRD and SEM, and the corresponding results are shown in Figure 14. The precipitate was cobalt oxalate, and its morphology exhibited thinly sliced and agglomerated particles.

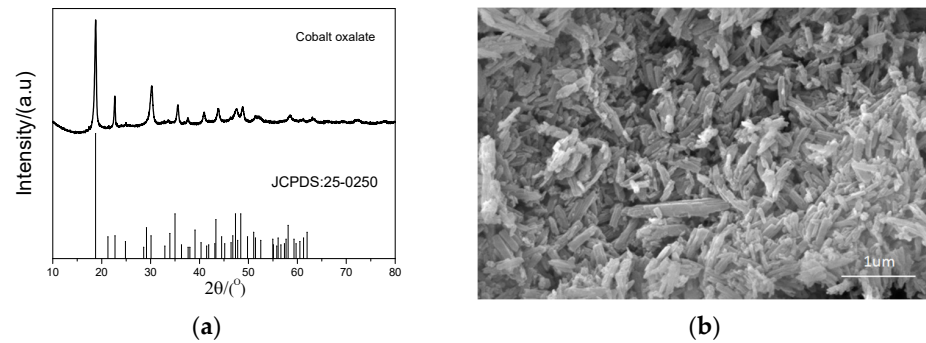


Figure 14. Characteristics of Co precipitate: (a) XRD pattern and (b) SEM image.

After extraction by a P507–N235 system under the optimal conditions, the raffinate contained Ni and Li. The addition of oxalic acid into the raffinate led to the formation of precipitate with the precipitation efficiency of 99%. XRD and SEM were used to analyze the precipitate. The results are shown in Figure 15. The precipitate phase was nickel oxalate with the granular morphology.

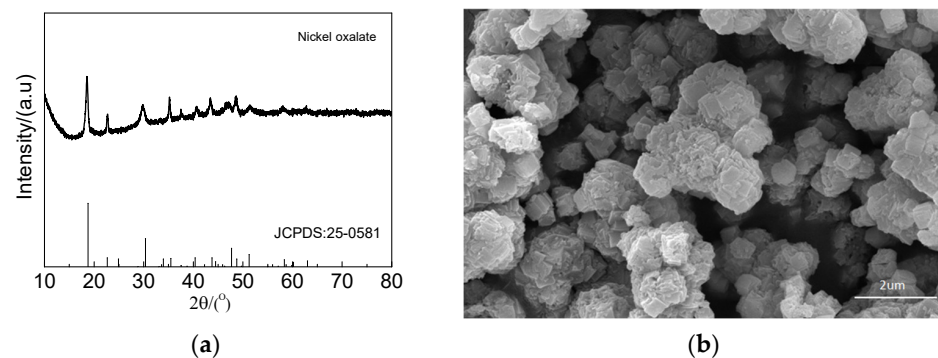


Figure 15. Characteristics of Ni precipitate: (a) XRD pattern and (b) SEM image.

Li in the raffinate was precipitated by sodium carbonate after Ni precipitation. The precipitation efficiency reached 98%. XRD and SEM were used to analyze the precipitate, and the results are shown in Figure 16. The precipitate phase was lithium carbonate, which consisted of granular particles.

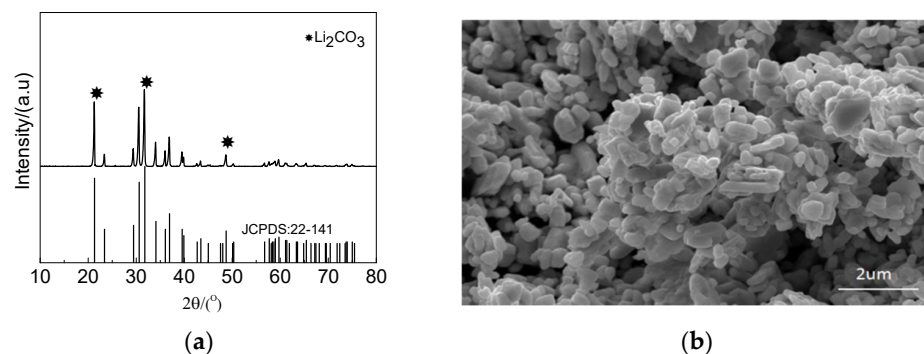


Figure 16. Characteristics of Li precipitate: (a) XRD pattern and (b) SEM image.

4. Conclusions

In this study, the separation and comprehensive recovery of valuable metallic elements, including Co, Ni, and Li, from spent power LIBs were realized by a hydrometallurgical process of “calcination–leaching–synergistic extraction–synthesis”. Based on the results, the following conclusions can be drawn:

- (1) The cathode active material was separated from the cathode plate of the spent power LIB with NaOH solution (2 mol L⁻¹) and then calcined at 700 °C to destroy the layered structure into NiO, CoO, and other substances. The calcined cathode active material was leached with sulfuric acid. The leaching efficiencies of Co, Ni, and Li were up to 100%.
- (2) A P204 system was selected to extract Al and Cu from the leaching solution. The results of the orthogonal experiment showed that the optimal parameters were pH = 4, saponification rate 50%, V_{P204}:V_{kerosene} = 1:2, and V_o:V_a = 1:2; the extraction efficiency of Al and Cu was 91% and 90%, respectively.
- (3) A P507–N235 non-saponification system was selected to extract Co. Under the conditions of V_{P507}:V_{N235} = 3:7, V_{P507-N235}:V_{kerosene} = 1:3, V_o:V_a = 4:1, and pH = 2.5, the maximum synergistic coefficient was 12.6; the extraction efficiencies of Co, Ni, and Li were 99.5%, 3.9%, and 9.7%, respectively. The separation coefficients of β_(Co/Ni) and β_(Co/Li) were 200.6 and 300.3, respectively.
- (4) After extraction with the P507–N235 system, pure cobalt oxalate, nickel oxalate, and lithium carbonate were obtained. Comprehensive recovery of valuable metals was realized with a total recovery efficiency of Li, Ni, and Co of 84.1%, 93.1%, and 96.5%, respectively. This process of “calcination–leaching–synergistic extraction–synthesis” is conducive to the enhancement of the extraction of Co, which has scientific and industrial technological significance for the recycling of the spent power LIBs.

Author Contributions: Methodology, L.M. and X.X.; investigation, Z.Z.; formal analysis, L.M. and Z.L.; writing—original draft preparation, Z.Z. and L.M.; writing—review and editing, L.M.; project administration, X.X.; funding acquisition, X.X. All authors have read and agreed to the published version of the manuscript.

Funding: This work was supported by the National Natural Science Foundation of China (52025042).

Data Availability Statement: The data presented in this study are available on request from the corresponding author.

Conflicts of Interest: The authors declare no conflict of interest.

References

1. Nguyen, T.H.A.; Oh, S.Y. Anode carbonaceous material recovered from spent lithium-ion batteries in electric vehicles for environmental application. *Waste Manag.* **2021**, *120*, 755–761. [[CrossRef](#)] [[PubMed](#)]
2. Zhao, S.; He, W.; Li, G. Recycling technology and principle of spent lithium-ion battery. In *Recycling of Spent Lithium-Ion Batteries Processing Methods and Environmental Impacts*; An, L., Ed.; Springer Nature: Berlin/Heidelberg, Germany, 2019; pp. 1–26.
3. Zhang, G.; Yuan, X.; He, Y.; Wang, H.; Zhang, T.; Xie, W. Recent advances in pretreating technology for recycling valuable metals from spent lithium-ion batteries. *J. Hazard. Mater.* **2021**, *406*, 124332. [[CrossRef](#)] [[PubMed](#)]
4. Lei, S.; Cao, Y.; Cao, X.; Sun, W.; Yang, Y. Separation of lithium and transition metals from leachate of spent lithiumion batteries by solvent extraction method with Versatic 10. *Sep. Purif. Technol.* **2020**, *250*, 117258.
5. Liu, C.; Lin, J.; Cao, H.; Sun, Z. Recycling of spent lithium-ion batteries in view of lithium recovery: A critical review. *J. Clean. Prod.* **2019**, *228*, 801–813. [[CrossRef](#)]
6. Makuza, B.; Tian, Q.; Guo, X.; Chattopadhyay, K.; Yu, D. Pyrometallurgical options for recycling spent lithium-ion batteries: A comprehensive review. *J. Power Sources* **2021**, *491*, 229622. [[CrossRef](#)]
7. Vanderbruggen, A.; Salces, A.; Ferreira, A.; Rudolph, M.; Serna-Guerrero, R. Improving separation efficiency in end-of-life lithium-ion batteries flotation using attrition pre-treatment. *Minerals* **2022**, *12*, 72. [[CrossRef](#)]
8. Yang, C.; Zhang, J.; Yu, B.; Huang, H.; Chen, Y.; Wang, C. Recovery of valuable metals from spent LiNi_xCo_yMn_zO₂ cathode material via phase transformation and stepwise leaching. *Sep. Purif. Technol.* **2021**, *267*, 118609. [[CrossRef](#)]
9. Jha, M.K.; Choubey, P.K.; Dinkar, O.S.; Panda, R.; Jyothi, R.K.; Yoo, K.; Park, I. Recovery of rare earth metals (REMs) from nickel metal hydride batteries of electric vehicles. *Minerals* **2022**, *12*, 34. [[CrossRef](#)]

10. Mousa, E.; Hu, X.; Ye, G. Effect of graphite on the recovery of valuable metals from spent Li-Ion batteries in baths of hot metal and steel. *Recycling* **2022**, *7*, 5. [[CrossRef](#)]
11. Nayaka, G.P.; Manjanna, J.; Pai, K.V.; Vadavi, R.; Keny, S.J.; Tripathi, V.S. Recovery of valuable metal ions from the spent lithium-ion battery using aqueous mixture of mild organic acids as alternative to mineral acids. *Hydrometallurgy* **2015**, *151*, 73–77. [[CrossRef](#)]
12. Zhang, Z.; Ma, L.; Zhang, X.; Wang, Y.; Cai, Y.; Xi, X. Acid leaching process of waste power lithium ion battery. In *Chinese Materials Conference CMC 2017: Advances in Energy and Environmental Materials*; Springer: Berlin/Heidelberg, Germany, 2018; pp. 657–665.
13. Jung, J.C.Y.; Sui, P.C.; Zhang, J.J. A review of recycling spent lithium-ion battery cathode materials using hydrometallurgical treatments. *J. Energy Storage* **2021**, *35*, 102217. [[CrossRef](#)]
14. Lei, S.; Sun, W.; Yang, Y. Solvent extraction for recycling of spent lithium-ion batteries. *J. Hazard. Mater.* **2022**, *424*, 127654. [[CrossRef](#)] [[PubMed](#)]
15. Ma, L.; Nie, Z.; Xi, X.; Han, X. Cobalt recovery from cobalt-bearing waste in sulphuric and citric acid systems. *Hydrometallurgy* **2013**, *136*, 1–7. [[CrossRef](#)]
16. Keller, A.; Hlawitschka, M.W.; Bart, H.J. Application of saponified D2EHPA for the selective extraction of manganese from spent lithium-ion batteries. *Chem. Process* **2022**, *171*, 108552. [[CrossRef](#)]
17. Joo, S.H.; Shin, D.; Oh, C.H.; Wang, J.P.; Senanayake, G.; Shin, S.M. Selective extraction and separation of nickel from cobalt, manganese and lithium in pre-treated leach liquors of ternary cathode material of spent lithium-ion batteries using synergism caused by Versatic 10 acid and LIX 84-I. *Hydrometallurgy* **2016**, *159*, 65–74. [[CrossRef](#)]
18. Qiu, Y.; Yang, L.; Huang, S.; Ji, Z.; Li, Y. The separation and recovery of copper(II), nickel(II), cobalt(II), zinc(II), and cadmium(II) in a sulfate-based solution using a mixture of Versatic 10 acid and Mextral 984H. *Chin. J. Chem. Eng.* **2017**, *25*, 760–767. [[CrossRef](#)]
19. Zhao, J.M.; Shen, X.Y.; Deng, F.L.; Wang, F.C.; Wu, Y.; Liu, H.Z. Synergistic extraction and separation of valuable metals from waste cathodic material of lithium ion batteries using Cyanex272 and PC-88A. *Sep. Purif. Technol.* **2011**, *78*, 345–351. [[CrossRef](#)]
20. Sun, Q.; Yang, L.; Huang, S.; Xu, Z.; Li, Y.; Wang, W. Synergistic solvent extraction of nickel by 2-hydroxy-5-nonylaceto-phenone oxime mixed with neodecanoic acid and bis(2-ethylhexyl) phosphoric acid: Stoichiometry and structure investigation. *Miner. Eng.* **2019**, *132*, 284–292. [[CrossRef](#)]
21. Li, H.; Feng, Y.; Wang, H.; Li, H.; Wu, H. Separation of V (V) and Mo (VI) in roasting-water leaching solution of spent hydrodesulfurization catalyst by co-extraction using P507-N235 extractant. *Sep. Purif. Technol.* **2020**, *248*, 117135. [[CrossRef](#)]
22. Xiong, P.; Zhang, Y.; Huang, J.; Bao, S.; Yang, X.; Shen, C. High-efficient and selective extraction of vanadium (V) with N235-P507 synergistic extraction system. *Chem. Eng. Res. Des.* **2017**, *120*, 284–290. [[CrossRef](#)]
23. Sun, X.; Sun, Y.; Yu, J. Removal of ferric ions from aluminum solutions by solvent extraction, part I: Iron removal. *Sep. Purif. Technol.* **2016**, *159*, 18–22. [[CrossRef](#)]
24. Cheng, C.Y.; Barnard, K.R.; Zhang, W.; Zhu, Z.; Pranolo, Y. Recovery of nickel, cobalt, copper and zinc in sulphate and chloride solutions using synergistic solvent extraction. *Chin. J. Chem. Eng.* **2016**, *24*, 237–248. [[CrossRef](#)]
25. Yang, Y.; Deng, S.; Lan, Q.; Nie, H.; Ye, X. The rare earth extraction and separation performance in P507-N235 system. *Nonferr. Metal. Sci. Eng.* **2013**, *4*, 83–86.
26. Yang, Y.; Lan, Q.; Deng, S.; Nie, H.; Ye, X. Chemical stability of P507-N235 and its synergistic extraction for NdCl₃. *J. Chin. Soc. Rare Earths* **2013**, *31*, 385–389.
27. Wang, Y.; Ma, L.; Xi, X.; Nie, Z.; Zhang, Y.; Wen, X.; Lyu, Z. Regeneration and characterization of LiNi_{0.8}Co_{0.15}Al_{0.05}O₂ cathode material from spent power lithium-ion batteries. *Waste Manag.* **2019**, *95*, 192–200. [[CrossRef](#)]
28. Guo, X.; Liu, J.; Dai, L.; Huang, L.; Wei, A.; He, Y.; Fang, D. Orthogonal wear experiment of 13Cr-L80 tubing string in high-yield gas wells and analysis of its influencing factors. *Eng. Fail. Anal.* **2021**, *125*, 105432. [[CrossRef](#)]
29. Hong, J.; Qian, Y.; Zhang, L.; Huang, H.; Jiang, M.; Yan, J. Laser nitriding of Zr-based metallic glass: An investigation by orthogonal experiments. *Surf. Coat. Technol.* **2021**, *424*, 127657. [[CrossRef](#)]
30. Liu, K.; Long, H.; Wang, Y.; Tang, X. Separation of cobalt and nickel from sulfate media using P507-N235 system. *Sep. Sci. Technol.* **2017**, *53*, 36–43. [[CrossRef](#)]